Journal of Alloys and Compounds 514 (2012) 1–5

Contents lists available at SciVerse ScienceDirect

Journal of Alloys and Compounds

journal homepage: www.elsevier.com/locate/jallcom

Letter

A novel low temperature synthesis route for $SmFeAsO_{1-x}F_x$ bulk superconductor with improved transport properties

J.B. Anooja, P.M. Aswathy, P.M. Sarun, U. Syamaprasad*

National Institute for Interdisciplinary Science and Technology (CSIR), Trivandrum 695019, India

ARTICLE INFO

Article history:
Received 29 July 2011
Received in revised form 19 October 2011
Accepted 8 November 2011
Available online 17 November 2011

Keywords:
Superconductors
Solid state reactions
Electrical transport
X-ray diffraction

ABSTRACT

Polycrystalline bulk samples of $SmFeAsO_{1-x}F_x$ with $0 \le x \le 0.4$ are synthesized at a temperature as low as 850 °C using a partially reacted precursor. The temperature dependence of resistivity and ac susceptibility measurements show superconducting transitions for all the fluorine doped samples and a T_C of 55.3 K, is observed for the sample with $x = 0.4$, processed at such a lower temperature. Moreover, for the first time, a transport J_C (752 A/cm^2 at 12 K) is measured in optimized bulk samples ($x = 0.3$) synthesized at 850 °C and ambient pressure. The new synthesis route which drastically reduces the processing temperatures can be of great use for conductor applications in respect of fluorine doped rare earth iron oxypnictides in general and Sm1111 in particular.

1. Introduction

The discovery of superconductivity in iron pnictides generated tremendous interest because of their relatively high critical temperature (T_C) up to 55 K [1–6] and very high upper critical field (H_{C2}) up to around 300 T [7,8]. Iron-based superconductors are the first non-cuprate materials exhibiting superconductivity at relatively high temperatures upon electron or hole doping of non-superconducting antiferromagnetic parent compounds. The versatility of this comprehensive class of superconductors lies in the possibility for any site substitution. The rare earth element substitution alone causes an enhancement of T_C more than double to that of the first reported La-based oxypnictide. Among the different rare-earth iron-oxypnictides, $SmFeAsO_{1-x}F_x$ (Sm1111) system is considered to be much promising due to its high T_C [6], relatively high H_{C2} [9] and significant intergrain current density [10]. Considering the methods of synthesis followed for polycrystalline iron oxypnictides, both ambient pressure and high pressure techniques have been employed. Generally, fluorine doped rare-earth (RE) iron-oxypnictides (RE1111) in bulk form are prepared by the so-called two-step method wherein FeAs and REAs are prepared in the first step and are added to the remaining ingredients in the second step in order to reduce volatile loss of As [11–15]. However, the method demands high temperature (>1150 °C) or high pressure (~6 GPa) to obtain good quality samples. Processing at elevated temperatures not only consumes more energy but also quite often leads to reaction of the sample with the container (mainly quartz) [16,17]. In this paper, we report a simple route to synthesize Sm1111 superconductor in bulk form which mitigates the above problems and provides good quality samples at a significantly low temperature of 850 °C. We could also measure a transport J_C of 752 A/cm^2 at 12 K which is quite motivating for a bulk sample synthesized at ambient pressures and without the support of any expensive barrier materials like Nb, Ta and Ag.

2. Experimental details

The synthesis method is essentially a single step process, i.e. all the ingredients are processed together. However, the heat treatment was done in two stages. Samples with nominal compositions of $SmFeAsO_{1-x}F_x$ ($x = 0$, 0.1, 0.2, 0.3, and 0.4) were synthesized by this method. Stoichiometric amounts of Sm, Fe, As, Fe_2O_3 and FeF_2 powders (M/s Alfa Aesar, purity 99.9%) were weighed, mixed and ground (inside a glove box with high purity argon atmosphere) to form a homogenous mixture. These samples were compacted into rectangular pellets with dimensions of 15 mm × 5 mm × 2 mm, under a pressure of 500 MPa. The pellets were barely placed in evacuated sealed quartz tubes. The sealed tubes were subjected to heat treatment at 370 °C for 5 h in a programmable muffle furnace having stability and accuracy better than ±1 °C controlled using Eurotherm-2404 temperature controller. This pre-processing temperature was chosen after monitoring the appearance of samples heat treated at temperatures ranging from 300 to 400 °C with an interval of 10 °C. The optimally pre-processed samples (360–380 °C) were again ground, re-pelletized and sealed in an evacuated quartz tube for the final sintering at 850 °C for 50 h.

The phase identification of the samples was performed using an X-ray diffractometer (Philips X'Pert Pro) with Cu Kα radiation employing a proprietary high speed detector and a monochromator at the diffracted beam side. Microstructural examination was done using a scanning electron microscope (JEOL-JSM-5600LV). Superconducting transport measurements such as resistivity versus temperature (ρ–T) and current versus voltage (I–V) were carried out using a closed-cycle

* Corresponding author. Tel.: +91 4712515373; fax: +91 4712491712.
E-mail address: syamcsir@gmail.com (U. Syamaprasad).

0925-8388/$ – see front matter © 2011 Published by Elsevier B.V.
doi:10.1016/j.jallcom.2011.11.041

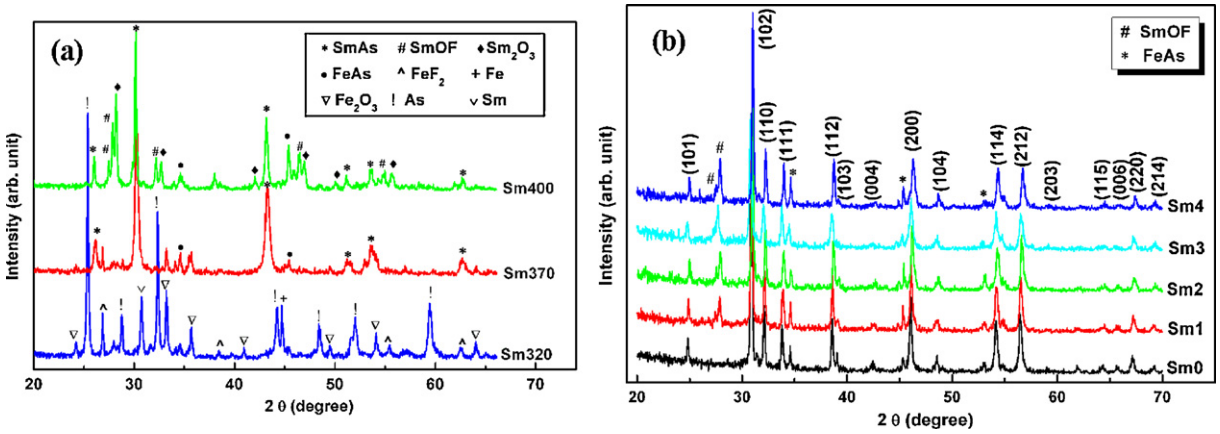

Fig. 1. (a) XRD patterns of pre-processed Sm1111 at 320, 370 and 400 °C. (b) XRD patterns of the Sm1111 with different doping levels of fluorine. The peaks of $SmFeAsO_{1-x}F_x$ are indexed.

cryocooler integrated-cryostat by DC four-probe technique. The temperature dependence of ac susceptibility (χ–T) was measured using a closed-cycle ac-susceptometer. The temperature of the sample was precisely controlled and monitored using two temperature controllers (Lakeshore-340&332) employing DT-670B-CU and DT-670A-SD sensors.

3. Results and discussion

Analysis of the samples processed in the first stage at temperatures in the range 300–400 °C shows that they can be categorized into three types depending on their color, shape and phase assemblage. The samples processed at 300–350 °C remain intact without much change in the original reddish color and shape. XRD analysis of a typical sample from this batch processed at 320 °C shows that the sample does not undergo any reaction (Fig. 1a Sm320). Whereas, the samples processed in the range 360–380 °C deform into brown powders with *in situ* formation of SmAs and minor quantities of FeAs and Sm_2O_3 (Fig. 1a Sm370). At temperatures above 380 °C, the major part of the sample fuses into metallic globules which stick to the surface of the quartz tube and some part remains as powder along with an arsenic coating on the inner surface of the tube. Neither the fused mass nor the As coating could be fully retrieved for further processing. XRD analysis of the fused mass shows the disappearance of Fe, FeF_2 and Fe_2O_3 and formation of SmOF along with an increase in Sm_2O_3 content (Fig. 1a Sm400). Fig. 2a–c shows photographs of the above three categories of samples. Further investigation has shown that the second category of powder (processed at 360–380 °C) is an appropriate precursor for the second stage processing.

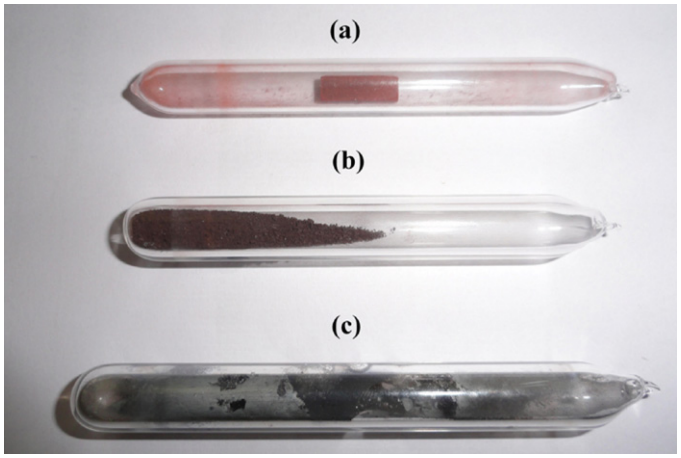

Fig. 2. Photographs of pre-processed Sm1111 at (a) 320 °C, (b) 370 °C and (c) 400 °C.

The second stage processing of the second category of precursor at 850 °C (50 h) yielded clean, black and dense rectangular pellets. No partial melting or globule formation is found during the processing. Fig. 1b shows the XRD patterns of Sm1111 samples with fluorine content $x = 0$, 0.1, 0.2, 0.3 and 0.4 labeled as Sm0, Sm1, Sm2, Sm3 and Sm4 respectively. Analysis of the patterns reveals that all samples contain $SmFeAsO_{1-x}F_x$ as the major phase confirming the formation of iron pnictides at temperatures as low as 850 °C. All the major peaks can be well indexed based on the tetragonal ZrCuSiAs type structure with the space group P4/nmm. The parental compound (Sm0) contains small quantities of FeAs along with the major phase. In addition to the main phase and FeAs, the fluorine doped samples contain SmOF also which increases with increase in the nominal composition of fluorine, while FeAs remains almost unchanged. Quantitative phase analysis of the samples was also done from the XRD data using the formula; vol.% of phase $X = (\sum$ Integrated peak intensities of phase $X)/(\sum$ Integrated peak intensities of all phases), and the data is given in Table 1. It is seen that the sample Sm0 contains Sm1111 phase as high as 92.9 vol.% while presence of secondary phases such as SmOF and FeAs reduces the volume-fraction of Sm1111 phase in the fluorine doped samples. These secondary phases are normally observed even in samples processed at temperatures above 1150 °C [2,13,18,19]. However, in the present case the volume-fraction of these phases are slightly higher than those synthesized at higher temperatures.

Fig. 3a shows ρ–T plots for the pure and fluorine doped samples. The temperature dependence of resistivity shows exactly similar characteristics as the previous reports [19,20]. An anomalous peak associated with structural transition and spin density wave instability is observed around 150 K in Sm0 [19–21]. But fluorine doping leads to a gradual suppression of the anomalous peak and its shifting to lower temperatures. The resistivity in the anomalous region drops for Sm1, but still there exists a trace of the anomaly. The substitution of fluorine for oxygen introduces charge carriers into the Fe–As layers and suppresses the phase transition. The anomalous behavior of the ρ–T plot is completely suppressed in the samples with $x > 0.2$, and the normal state resistivity decreases linearly with the emergence of superconductivity. A $T_{C\text{-onset}}$ of 55.3 K is obtained for Sm4. Such high transition temperatures have already been reported for this system processed above 1160 °C, but we could achieve the same at 850 °C. The $T_{C\text{-onset}}$ of samples Sm0, Sm1, Sm2 and Sm3 are found to be 20.1, 38.1 and 53.4 K respectively. The $T_{C\text{-offset}}$ of Sm1 is below 11 K which is beyond the limit of the

Table 1
Different parameters observed for Sm1111 with different fluorine contents.

Sample name	Vol.%. of phases			T_C (K) from		ΔT_C (K)	RRR	I_C (A)	J_C (A/cm^2)
	Pure	SmOF	FeAs	ρ–T	χ–T				
Sm0	92.9	0	7.1	–	–	–	–	–	–
Sm1	84.6	6.5	8.9	20.1	18	–	1.98	–	–
Sm2	83.3	8.1	8.6	38.1	35	5.7	2.34	7.3	182
Sm3	80.7	10.4	8.9	53.4	51.3	4.3	5.51	30.1	752
Sm4	80.6	10.3	9.1	55.3	52	7.2	4.66	19.8	495

measurement system. Therefore, the ΔT_C has been measured only for Sm2, Sm3 and Sm4 which is given in Table 1. The residual resistivity ratio (RRR = ρ_{300}/ρ_{60}) estimated for all the superconducting samples is included in Table 1. These RRR values are lesser than La1111 system indicating stronger impurity scattering similar to previous reports [22]. The transition temperatures were also determined from ac susceptibility measurement (Table 1) which is in agreement with those obtained from ρ–T plot. A typical χ–T plot for the sample Sm3 is shown in Fig. 3c. One can easily distinguish two steps in the real part of χ–T; the step near T_C is due to the superconducting-grain shielding, while that at lower temperature to the intergrain shielding. Corresponding to the low-T step, there is a well-defined peak in the imaginary part of χ–T, while the expected near-T_C peak is not well resolved. A double step in the real part of the χ–T plot is a known feature of a granular magnetic response which is consistent with the previous reports on iron oxypnictides [23]. It is well accepted that inhomogeneous superconductors also exhibit such features and this has been discussed for Sm1111 as well [24,25]. Hence, the observed extended diamagnetic transition along with the double step feature can be considered as a combined effect of the presence of secondary phases and the electromagnetic granularity of the sample.

In order to determine the current carrying capacity of the samples we measured the self-field transport I_C using a criterion of 1 μV/cm from I–V characteristics. The transport J_C values at 12 K for all the samples are listed in the Table 1 which shows that J_C is maximum (752 A/cm^2) for Sm3 having a doping concentration of $x = 0.3$. The J_C of Sm4 sample which exhibited the highest T_C is found to be lower (495 A/cm^2) than Sm3. The I–V plot for the sample with the maximum I_C (Sm3) is shown in Fig. 3b.

The microstructural analysis of all the fluorine doped samples was performed using SEM. Fig. 4 shows the SEM images of freshly fractured surfaces of Sm1, Sm2, Sm3 and Sm4 pellets respectively. The images show that the microstructure is almost homogeneous with some voids. An improvement in grain size and a decrease in porosity can be observed as the fluorine content increases from Sm1 to Sm3. However, the porosity increases from Sm3 to Sm4. Thus, it can be inferred that the increased grain size and reduced porosity are responsible for the higher J_C observed in Sm3 compared to Sm4 though the latter exhibits higher T_C.

The choices of the phase assemblage of a precursor and the reactivity of its individual phases have major roles in the preparation of any complex compound through solid-state route. The final phase purity, processing temperature and duration mainly depend on the above factors. In the present work, the pre-processing of the reaction mixture at an optimized temperature range of 360–380 °C has probably yielded a precursor having the right phase assemblage and good reactivity. The precursor has not been allowed to undergo fusion, but the temperature is tuned such that reacted binary phases such as SmAs and FeAs are formed *in situ*. These phases will have higher reactivity compared to those used for two-step process in which these are usually prepared separately at a higher temperature of 500–900 °C [12–15]. Moreover, since the pre-processed precursor is given an intermediate grinding before the final heat treatment, the metallic particles fully disperse in the matrix and hence do not agglomerate or fuse together; but only increases the reactivity. This may be the main reason for achieving good quality fluorine doped Sm1111 samples at a temperature as low as 850 °C. It is to be noted that the samples subjected to the second stage heat treatment are not wrapped with any expensive

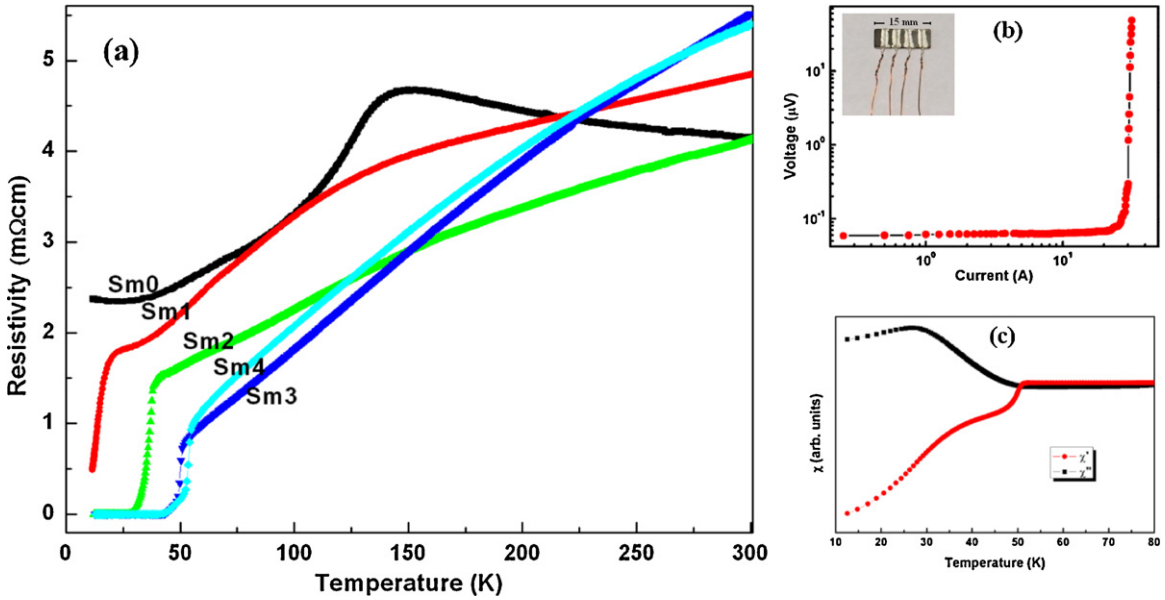

Fig. 3. (a) The resistivity versus temperature plot for various fluorine doped samples, (b) I–V plot (inset shows the photograph of the sample used for four probe measurement) and (c) the ac susceptibility versus temperature plot of sample Sm3.

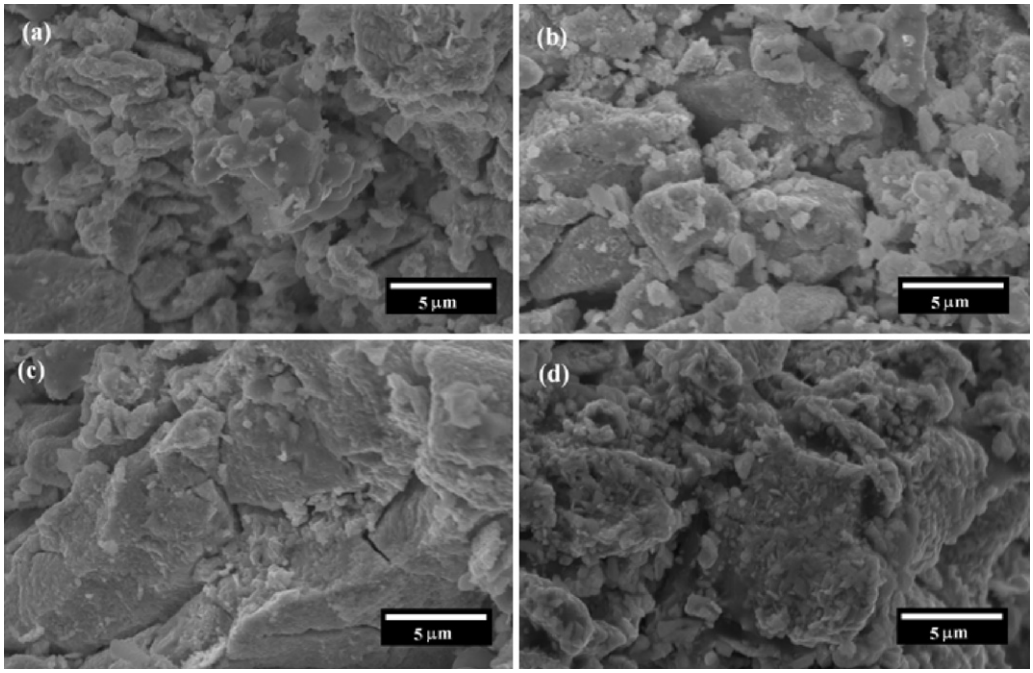

Fig. 4. SEM images of the fractured surfaces of (a) Sm1, (b) Sm2, (c) Sm3 and (d) Sm4.

metallic foil as has been usually done for the two-step process, yet clean pellets devoid of any reaction with quartz tube have been obtained. Another important feature is the measurement of a significant value of transport J_C through the samples processed by the present method. To the best of our knowledge, this is the first report of obtaining Sm1111 bulk superconducting samples processed at ambient pressure which can carry significant transport J_C. The process needs further refinement in order to enhance phase purity, microstructure and hence the transport J_C. Apart from the bulk sample preparation, this synthesis route can also be a solution for the major obstacle, i.e. reaction of the sheath metal with the reaction mixture especially with the RE and As, in the development of iron pnictide wires [26]. Since the pre-processed precursor does not have any free RE or As, their reactivity with the sheath material will be drastically reduced and hence there is a great scope for using inexpensive metals in the fabrication of iron pnictide wires. Currently, the attempt to measure transport J_C is proved to be successful only in silver sheathed conductors [27].

4. Conclusion

$SmFeAsO_{1-x}F_x$ superconducting bulk samples were synthesized at a significantly low temperature of 850 °C by introducing a novel pre-processing step. The samples prepared at such low temperatures and ambient pressure show a T_C of 55.3 K, which has been observed earlier only for samples processed at high temperatures or pressures. Further a transport J_C (752 A/cm^2 at 12 K) has been measured for the fluorine doped Sm1111 bulk sample. The main advantage is that it is not necessary to afford high temperatures and pressures or expensive sheath materials for the synthesis of iron-oxypnictide polycrystalline bulk samples. The synthesis route detailed herein can help in surpassing the hurdles for the future development of iron-pnictide conductors.

Acknowledgments

JB Anooja and PM Aswathy acknowledge the Kerala State Council for Science, Technology and Environment (KSCSTE) and PM Sarun acknowledges the Council of Scientific and Industrial Research (CSIR) for their Research Fellowships.

References

[1] Y. Kamihara, T. Watanabe, M. Hirano, H. Hosono, J. Am. Chem. Soc. 130 (2008) 3296–3297.
[2] X.H. Chen, T. Wu, G. Wu, R.H. Liu, H. Chen, D.F. Fang, Nature 453 (2008) 761–762.
[3] P.M. Aswathy, J.B. Anooja, P.M. Sarun, U. Syamaprasad, Supercond. Sci. Technol. 23 (073001 (Topical Review)) (2010) 20.
[4] Z.A. Ren, J. Yang, W. Lu, W. Yi, X.L. Shen, Z.C. Li, G.C. Che, X.L. Dong, L.L. Sun, F. Zhou, Z.X. Zhao, Europhys. Lett. 82 (57002) (2008) 2.
[5] J. Yang, Z.C. Li, W. Lu, W. Yi, X.L. Shen, Z.A. Ren, G.C. Che, X.L. Dong, L.L. Sun, F. Zhou, Supercond. Sci. Technol. 21 (82001) (2008) 3.
[6] Z.A. Ren, W. Lu, J. Yang, W. Yi, X.L. Shen, Z.C. Li, G.C. Che, X.L. Dong, L.L. Sun, F. Zhou, Z.X. Zhao, Chin. Phys. Lett. 25 (2008) 2215–2216.
[7] J. Jaroszynski, F. Hunte, L. Balicas, Y.J. Jo, I. Raičević, A. Gurevich, D.C. Larbalestier, F.F. Balakirev, L. Fang, P. Cheng, Y. Jia, H.H. Wen, Phys. Rev. B 78 (174523) (2008) 9.
[8] Y. Jia, P. Cheng, L. Fang, H. Luo, H. Yang, C. Ren, L. Shan, C. Gu, H.H. Wen, Appl. Phys. Lett. 93 (032503) (2008) 3.
[9] C. Senatore, R. Flukiger, M. Cantoni, G. Wu, R.H. Liu, X.H. Chen, Phys. Rev. B 78 (054514) (2008) 7.
[10] A. Yamamoto, A.A. Polyanskii, J. Jiang, F. Kametani, C. Tarantini, F. Hunte, J. Jaroszynski, E.E. Hellstrom, P.J. Lee, A. Gurevich, D.C. Larbalestier, Z.A. Ren, J. Yang, X.L. Dong, W. Lu, Z.X. Zhao, Supercond. Sci. Technol. 21 (095008) (2008) 11.
[11] G.F. Chen, Z. Li, D. Wu, G. Li, W.Z. Hu, J. Dong, P. Zheng, J.L. Luo, N.L. Wang, Phys. Rev. Lett. 100 (247002) (2008) 4.
[12] B. Lorenz, K. Sasmal, R.P. Chaudhury, X.H. Chen, R.H. Liu, T. Wu, C.W. Chu, Phys. Rev. B 78 (012505) (2008) 4.
[13] A. Martinelli, M. Ferretti, P. Manfrinetti, A. Palenzona, M. Tropeano, M.R. Cimberle, C. Ferdeghini, R. Valle, C. Bernini, M. Putti, A.S. Siri, Supercond. Sci. Technol. 21 (095017) (2008) 7.
[14] L. Wang, Z. Gao, Y. Qi, X. Zhang, D. Wang, Y. Ma, Supercond. Sci. Technol. 22 (015019) (2009) 6.
[15] F. Kametani, P. Li, D. Abraimov, A.A. Polyanskii, A. Yamamoto, J. Jiang, E.E. Hellstrom, A. Gurevich, D.C. Larbalestier, Z.A. Ren, J. Yang, X.L. Dong, W. Lu, Z.X. Zhao, Appl. Phys. Lett. 95 (142502) (2009) 3.
[16] H. Takahashi, K. Igawa, K. Arii, Y. Kamihara, M. Hirano, H. Hosono, Nature 453 (2008) 376–378.
[17] Y.L. Chen, Y.J. Cui, C.H. Cheng, Y. Yang, L. Wang, Y.C. Li, Y. Zhang, Y. Zhao, Physica C 470 (2010) 989–992.
[18] Y. Kamihara, T. Nomura, M. Hirano, J. Eun Kim, K. Kato, M. Takata, Y. Kobayashi, S. Kitao, S. Higashitaniguchi, Y. Yoda, M. Seto, H. Hosono, New J. Phys 12 (033005) (2010) 14.
[19] J. Yang, Z.A. Ren, G.C. Che, W. Lu, X.L. Shen, Z.C. Li, W. Yi, X.L. Dong, L.L. Sun, F. Zhou, Z.X. Zhao, Supercond. Sci. Technol. 22 (025004) (2009) 5.

[20] R.H. Liu, G. Wu, T. Wu, D.F. Fang, H. Chen, S.Y. Li, K. Liu, Y.L. Xie, X.F. Wang, R.L. Yang, L. Ding, C. He, D.L. Feng, X.H. Chen, Phys. Rev. Lett. 101 (087001) (2008) 4.
[21] S. Margadonna, Y. Takabayashi, M.T. McDonald, M. Brunelli, G. Wu, R.H. Liu, X.H. Chen, K. Prassides, Phys. Rev. B 79 (014503) (2009) 7.
[22] A.S. Sefat, M.A. McGuire, B.C. Sales, R. Jin, J.Y. Howe, D. Mandrus, Phys. Rev. B 77 (174503) (2008) 6.
[23] M. Polichetti, M.G. Adesso, D. Zola, J.L. Luo, G.F. Chen, Z. Li, N.L. Wang, C. Noce, S. Pace, Phys. Rev. B 78 (224523) (2008) 10.
[24] L. Zhang, X. Leng, S.Y. Ding, X.B. Zhu, Y.P. Sun, Supercond. Sci. Technol. 23 (065020) (2010) 6.
[25] A. Yamamoto, J. Jiang, F. Kametani, A. Polyanskii, E. Hellstrom, D. Larbalestier, A. Martinelli, A. Palenzona, M. Tropeano, M. Putti, Supercond. Sci. Technol. 24 (045010) (2011) 7.
[26] X. Zhang, L. Wang, Y. Qi, D. Wang, Z. Gao, Z. Zhang, Y. Ma, Physica C 470 (2010) 104–108.
[27] L. Wang, Y. Qi, D. Wang, Z. Gao, X. Zhang, Z. Zhang, C. Wang, Y. Ma, Supercond. Sci. Technol. 23 (075005) (2010) 4.